European Journal of Medicinal Chemistry 63 (2013) 256–268

Contents lists available at SciVerse ScienceDirect

European Journal of Medicinal Chemistry

journal homepage: http://www.elsevier.com/locate/ejmech

Original article

Novel chiral ferrocenylpyrazolo[1,5-a][1,4]diazepin-4-one derivatives – Synthesis, characterization and inhibition against lung cancer cells

Shi-Li Shen [a], Jin-Hui Shao [b], Ji-Zhuang Luo [b], Jin-Ting Liu [a], Jun-Ying Miao [b,*], Bao-Xiang Zhao [a,*]

[a] Institute of Organic Chemistry, School of Chemistry and Chemical Engineering, Shandong University, Shanda Nanlu 27, Jinan, Shandong 250100, PR China
[b] Institute of Developmental Biology, School of Life Science, Shandong University, Shanda Nanlu 27, Jinan, Shandong 250100, PR China

ARTICLE INFO

Article history:
Received 24 October 2012
Received in revised form
19 January 2013
Accepted 13 February 2013
Available online 24 February 2013

Keywords:
Pyrazole
Ferrocene
Chiral diazepinone
Lung cancer cells
Cell cycle arrest
Apoptosis

ABSTRACT

A series of novel 2-ferrocenyl-7-hydroxy-5-phenethyl-5,6,7,8-tetrahydro-4*H*-pyrazolo[1,5-a][1,4]diazepin-4-one derivatives with optical activity (**2**) was synthesized in the microwave-assisted condition and characterized by means of IR, ^{1}H NMR and mass spectroscopy, and furthermore confirmed by X-ray analysis of a representative compound (*R*)-**2a**. Preliminary biological evaluation showed that some compounds could suppress the growth of A549, H322 and H1299 lung cancer cells. Among the tested compounds, **2b**–**d** were more effective and might perform their action through cell cycle arrest for A549 cell. Whereas these compounds inhibited growth of H1299 and H322 cells by inducing apoptosis. The anti-tumor activities of these compounds were related to the nature of substituents in benzene moiety. In addition, the results indicated also that compounds **2b**–**d** possessed notable cytotoxicity and selectivity for A549 vs H1299 and H322 lung cancer cells.

1. Introduction

Cancer is the second major cause of deaths after cardio and cerebrovascular diseases. Non-small cell lung cancer (NSCLC) accounts for 80% of lung cancers, and is the leading cause of cancer mortality. Overall, the 5-year survival rate of NSCLC patients is poor and hardly reaches 15%, due to NSCLC is relatively resistant to chemotherapy and radiation therapy [1,2]. Furthermore, the adverse effects of chemotherapeutic compounds often hamper the quality of life of lung cancer patients. Therefore, the discovery of effective novel prophylactic, diagnostic, and therapeutic treatments for NSCLC is urgently needed.

Pyrazole represents an important class of nitrogen-containing heterocycles and compounds with pyrazole framework display diverse biological activities such as anti-cancer, antimicrobial, antiinflammatory, antiangiogenic, antidepressant, antioxidant and antiinfluenza activities [3–9]. Recently, much attention has been focused on pyrazoles [10–15]. Pyrazole-containing structures have also been found among naturally occurring compounds such as the antibiotic pyrazofurin which has been documented to possess potent anti-cancer and antimicrobial activities [16].

Diazepanone ring is a core structure of the liposidomycins and caprazamycins which are unique nucleoside-type antibiotics isolated from *Streptomyces* [17–19]. These natural products have elicited intense interest in the scientific community because of their antibiotic properties. In addition to their striking antibiotic profiles, their complex and unprecedented molecular architectures have appealed to synthetic chemists to investigate these molecules as synthetic targets of great biological interest [20]. Various analogs of them have been synthesized and showed extent bioactivity such as anti-tuberculosis [21].

Metal-based complexes have been playing a prominent role in the medicinal chemistry and drug development since the discovery of the anti-tumor properties of square-planar platinum (II) complex (cisplatin) reported by Rosenberg et al. in 1969 [22]. Though platinum complex continue to play a central role in the treatment of patients suffering from cancer [23], they suffer from two main disadvantages: side effects such as nephrotoxicity and ineffectiveness against platinum-resistant tumors [24]. There is an urgent need to develop cisplatin analogs and design other new metal-based complexes. During the past years, numerous promising new organometallic complexes were reported to exhibit high anticancer activity, such as Au complexes [25,26], Rh complexes [27], Ru complexes [28,29], Ir complexes [30], Ti complexes [31,32], Os complexes [33], ferrocene derivatives [34,35] and so on. Among them, ferrocene derivatives have captured the attention of chemists

* Corresponding authors. Tel.: +86 531 88366425; fax: +86 531 88564464.
E-mail addresses: miaojy@sdu.edu.cn (J.-Y. Miao), bxzhao@sdu.edu.cn, sduzhao@hotmail.com (B.-X. Zhao).

0223-5234/$ – see front matter © 2013 Elsevier Masson SAS. All rights reserved.
http://dx.doi.org/10.1016/j.ejmech.2013.02.016

so intensively since the first report of ferrocene in 1951 [36]. Incorporation of a ferrocene fragment into a molecule of an organic compound often resulted in excellent biological activity due to its similarities in aromaticity, lipophilicity, and morphology to a phenyl ring, along with the unusual redox properties [37]. For example, ferroquine, which is obtained by the replacement of a CH_2 group with a ferrocenyl group in the anti-malarial chloroquine, is active against both chloroquine-sensitive and chloroquine-resistant *Plasmodium falciparum* [38], and is about to complete phase II clinical trials as a treatment for uncomplicated malaria [39]. In addition, the stability and non-toxicity of the ferrocene moiety is of particular interest rendering such drugs compatible with other treatment. A lot of ferrocenyl compounds display anti-tumor, antioxidant and antimycobacterial activity [40–43].

In an attempt to search for novel anti-tumor compounds, we focused our attention to the design, synthesis and bioactivity evaluation of pyrazole derivatives with structure diversity [44–57]. In a continuation of an ongoing program aiming at finding new structural leads with potential chemotherapeutic activities, it was rationalized to synthesize some novel pyrazole fused heterocycle that would produce anti-cancer activity. The design of pyrazolo-diazepanone scaffolds should be the most suitable plan to reach large families of compounds with structure diversity because it can take advantage of multiple functional groups which facilitate the further introduction of pharmacophoric groups. Furthermore, scaffolds with cyclic structures can reduce the entropic cost associated with the loss of conformational degrees of freedom upon binding to the target protein. We would like to report the synthesis of novel 2-ferrocenyl-7-hydroxy-5-phenethyl-5,6,7,8-tetrahydro-4*H*-pyrazolo[1,5-a][1,4]diazepin-4-one derivatives with optical activity by microwave-assisted reaction, and preliminary biological evaluation against A549, H322 and H1299 lung cancer cells.

2. Chemistry

2.1. Synthesis

The target compounds, 2-ferrocenyl-7-hydroxy-5-phenethyl-5,6,7,8-tetrahydro-4*H*-pyrazolo[1,5-a][1,4]diazepin-4-one derivatives, were synthesized by the reaction of (*R*) or (*S*)-3-ferrocenyl-1-(oxiran-2-ylmethyl)-1*H*-pyrazole-5-carboxylate **1** and 2-arylethanamine as outlined in Scheme 1. Starting materials (*R*) or (*S*)-**1** were easily obtained from ethyl 3-ferrocenyl-1*H*-pyrazole-5-carboxylate and (*R*)- or (*S*)-oxiran-2-ylmethyl 4-methylbenzenesulfonate according to previous reported method [14]. The synthesis was performed both under classical convective and microwave-assisted heating techniques. Firstly, the reaction was carried out under the condition of reflux in ethanol. Although desired compounds were obtained, the yields were lower (20–28%) because byproducts **3** and **4** were also formed as shown in Scheme 2. In order to prepare the target compounds in approving yields, the reaction was performed in a sealed tube under higher temperature (140 °C). As expected, the compounds were obtained in higher yield (62–82%).

Microwave-assisted chemistry has blossomed into a useful technique for a variety of applications in organic synthesis and inorganic synthesis. The use of microwave heating can dramatically cut down reaction time, increase product purity and yields, and allow precise control of reaction conditions. Thus, we focused our attention on the microwave-assisted synthesis technique after obtaining compounds **2** by classical heating method. These reactions are performed in a microwave synthesis lab station. In a typical experiment, ethyl 3-ferrocenyl-1-(oxiran-2-ylmethyl)-1*H*-pyrazole-5-carboxylate **1** and amine were mixed in an open vessel and irradiated keeping the reaction temperature at 70 °C for 10–15 min without any solvent. After work-up, desired compounds were obtained. Comparing two methods, microwave-assisted synthesis technique dramatically cut down reaction time, increase product yields as shown in Table 1. Similarly, we synthesized two compounds (*R*)-**5** and (*S*)-**5** with phenyl instead of ferrocene (Scheme 3) in order to compare effects of the compounds with and without ferrocene against lung cancer cells.

The structures of 2-ferrocenyl-7-hydroxy-5-phenethyl-5,6,7,8-tetrahydro-4*H*-pyrazolo[1,5-a][1,4]diazepin-4-one derivatives **2** were determined by IR, ^{1}H NMR and mass spectroscopy. For example, (*R*)-2-ferrocenyl-7-hydroxy-5-phenethyl-5,6,7,8-tetrahydro-4*H*-pyrazolo[1,5-a][1,4]diazepin-4-one ((*R*)-**2a**), obtained in 81% yield as yellow solid, gave a $[M + H]^+$-ion peak at *m*/*z* 456.1375 in HRMS in accord with the molecular formula $C_{25}H_{26}FeN_3O_2$ ($[M + H]^+$: 456.1374). In the IR spectra, the band at 3398 cm^{-1} is typical stretching vibration absorption of hydroxyl group. The two weak bands appeared at 2923 and 2869 cm^{-1} may

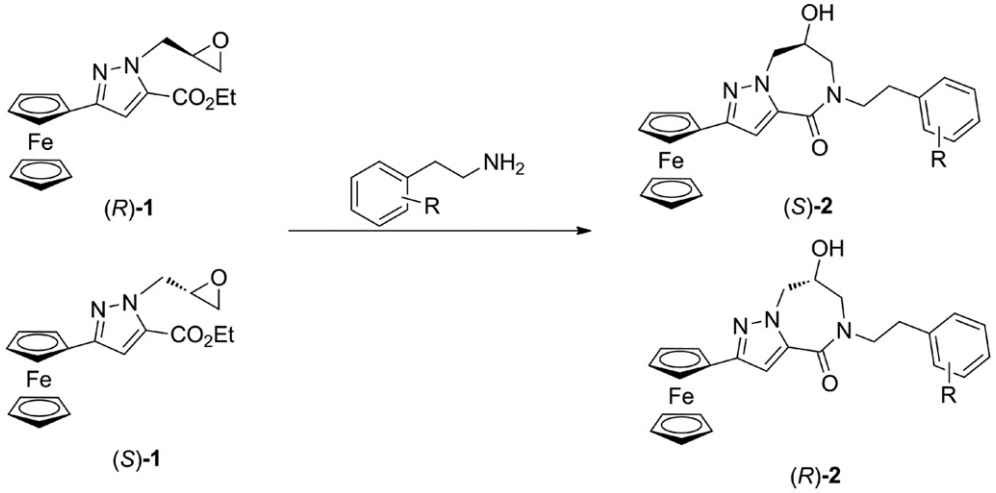

Scheme 1. Synthesis of pyrazolo[1,5-a][1,4]diazepin-4-one derivatives **2**.

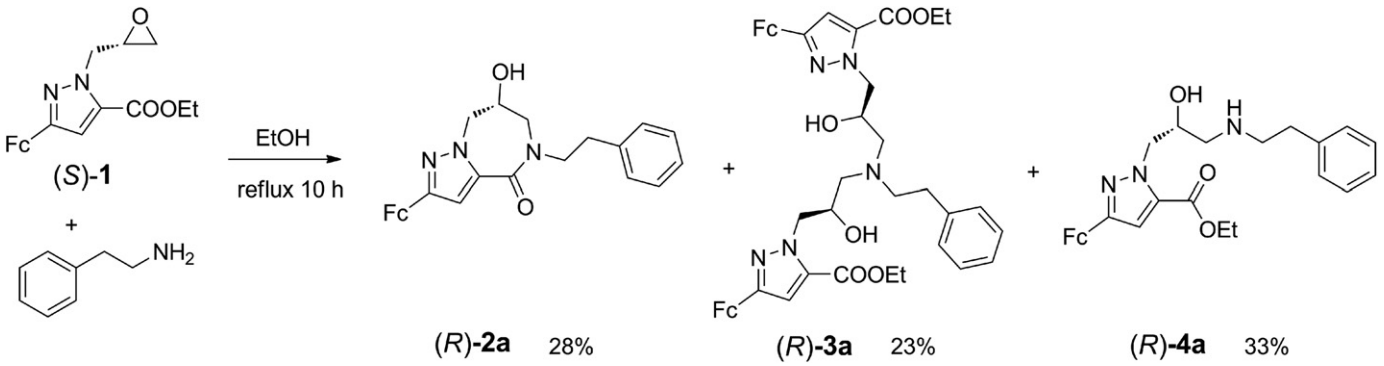

Scheme 2. The formation of byproducts **3** and **4**.

be ascribed to the C–H absorptions. The absorption of carbonyl group was observed at 1607 cm^{-1}, and the C=N absorption was observed at 1526 cm^{-1}. The torsional or swing vibration absorption of CpFeCp appeared at 484 cm^{-1}. The ^1H NMR spectra indicated chemical shift of the OH at δ = 5.47 ppm as doublet peaks (J = 3.9 Hz). One proton signal in pyrazole moiety appeared at δ = 6.82 ppm. The protons of one methylene in the phenethyl moiety appeared at δ = 2.92 ppm as triplet peaks (J = 7.5 Hz), the other methylene protons in the phenethyl moiety appeared at δ = 3.58 ppm (dt, J = 13.5 Hz, 7.5 Hz) and δ = 3.86 ppm (dt, J = 13.5 Hz, 7.5 Hz), respectively. Furthermore, the structure was confirmed by the X-ray diffraction as shown in Fig. 1.

2.2. Single-crystal structure

Single crystals of (*R*)-**2a** were all grown via slow evaporation of ethyl acetate solution. The molecular view of (*R*)-**2a** is shown in Fig. 1. Details of crystal data, data collection and refinement parameters are compiled in Tables 2 and 3.

Fig. 1 shows that (*R*)-**2a** contains a ferrocenyl bound to pyrazole ring which fused with diazepanone ring. All of the bond lengths and bond angles in pyrazole and diazepanone rings are in the normal range (Table 3). The dihedral angle between the substituted cyclopentadienyl (Cp) ring (C1–C5) and the pyrazole ring (N2/N3/C11/C12/C13) is 13.9(3) Å that is similar to that found in related structures [58]. The C5–C11 distance is 1.464(7) Å. While the phenyl ring (C20–C25) and the pyrazole ring in the molecule is nearly perpendicular with an angle of 87.0(3)°. The two methylene groups of the phenethyl moiety in **2a** were dually disordered at 298 K (Fig. 1) resulting in conformational synmorphism. The distribution of conformers A and B in the crystal is found in number ratio 0.60:0.40. The molecular conformation A is stabilized by intramolecular $C18_A–H18_B\cdots O1$ weak hydrogen bond (Fig. 1, Table 4).

Two Cp rings of the ferrocene fragment are perfectly planar but deviate slightly from being parallel with an angle of 1.9(4)° and are almost in the eclipsed conformation by the torsion angle C–Cg2–Cg3–C varies between −5.09 and −6.20°, where Cg2 and Cg3 are the substituted and unsubstituted Cp ring centroids, respectively. The Fe1–Cg2 and Fe1–Cg3 distances are 1.644(3) and 1.650(4) Å respectively, and the Cg2–Fe1–Cg3 angle is 178.75(17)°. The Fe–C distances in unsubstituted Cp ring are all similar to those found in ferrocene itself [59], ranging from 2.020(7) to 2.033(7) Å [mean 2.024(1) Å], while those in substituted Cp ring are different and range from 2.027(5) to 2.040(5) Å [mean 2.032(1) Å] (Table 3), thus indicating distortion of the ferrocene moiety caused by substitution at C5. The longest Fe–C5 distance of 2.040(5) Å shows displacement of the atom away from the Fe atom.

The seven-membered diazepanone ring displays a twisted boat conformation, the atoms of C14, C16, C17 and N3 form the bottom of the boat (Maximum deviation from the mean N3/C14/C16/C17 plane = 0.155 Å), C15 the prow, and N2 and C13 the stern [distances from the N3/C14/C16/C17 mean plane = 0.557, 0.813, 0.912 Å, respectively].

The crystal packing of structure (*R*)-**2a** was stabilized by strong intermolecular hydrogen bonds and weak C–H$\cdots\pi$ interactions (Table 4). In the crystal lattice, the carbonyl groups of the diazepanone interact with the hydroxy groups of the adjacent molecules through linear O2–H2$\cdots$O1 hydrogen bonds to form an infinite one-dimensional chain along the (100) direction. It is interesting to find that a pairs of $C17–H17_A\cdots Cg3$ hydrogen π interactions join the adjacent molecules into centrosymmetric $R22(16)$ dimers. Moreover, pairs of C–H$\cdots\pi$ interactions of the $C17–H17_A\cdots Cg4$ (Cg4 is the centroid of the benzene ring) join the dimers with one another to result in formation of the three-dimensional structure (Fig. 2).

Table 1
The yields of compounds **2** in three conditions.

Entry	Products	Classical heating[a]		In sealed tube[b]		Microwave-assisted[c]	
		Time (h)	Yields (%)	Time (h)	Yields (%)	Time (min)	Yields (%)
1	(*S*)-**2a**	10	25	10	74	10	81
2	(*S*)-**2b**	10	21	8	80	10	74
3	(*S*)-**2c**	10	21	12	65	15	72
4	(*S*)-**2d**	10	20	12	72	15	75
5	(*R*)-**2a**	10	28	10	78	10	81
6	(*R*)-**2b**	10	22	8	82	10	74
7	(*R*)-**2c**	10	20	12	62	15	74
8	(*R*)-**2d**	10	21	12	71	15	77

[a] Alcohol, reflux.
[b] Alcohol, 140 °C.
[c] No solvent, 70 °C.

2.3. Cyclic voltammetry

The electrochemical characterization of the synthesized compounds was performed by means of cyclic voltammetry (CV). The compounds (*R*)- and (*S*)-**2a**–**d** were dissolved in CH_2Cl_2 to give a solution containing 0.5 mM of the analyte and 0.1 M $Bu_4N[PF_6]$ as the supporting electrolyte. The redox properties of ferrocene derivatives are of particular interest as they have been implicated in the production of reactive oxygen species (ROS) responsible for their anti-cancer activity [60,61]. Meanwhile CV measurements provide an additional proof of purity of our biologically investigated compounds. Pertinent data are presented in Table 5. Fig. 3 shows the voltammograms of (*R*)- and (*S*)-**2a**–**d**.

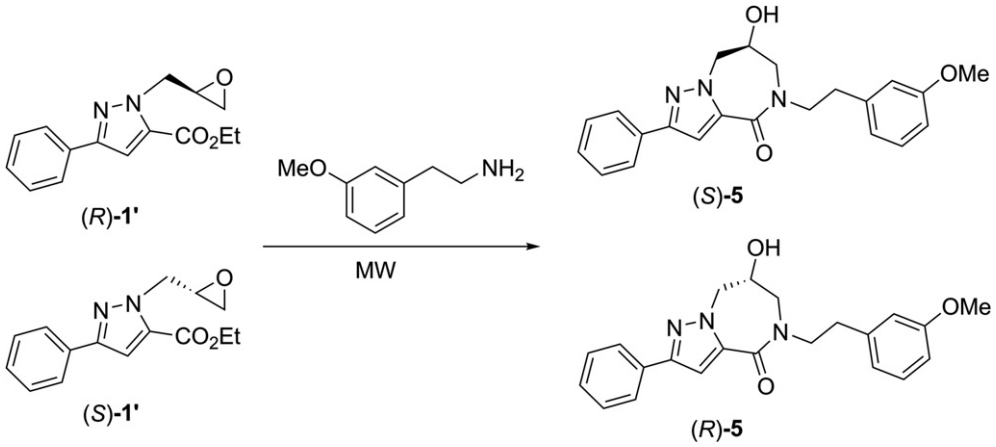

Scheme 3. Synthesis of pyrazolo[1,5-a][1,4]diazepin-4-one derivatives **5**.

Under the above-described experimental conditions, compounds (*R*)- and (*S*)-**2a**–**d** undergo one-electron oxidations at half-wave potentials of *ca.* 450 mV against the ferrocene/ferrocenium redox couple. As shown in Table 5, almost the same half-wave potentials of compounds (*R*)- and (*S*)-**2a**–**d** indicate that the different substituent in benzene moiety nearly don't have any influence on the redox properties due to the lack of electronic interactions between the ferrocenyl moiety and benzene moiety. The cyclic voltammetry behavior showed that the redox property of compounds (*R*)- and (*S*)-**2a**–**d** is similar to other ferrocene derivatives reported [62]. Moreover, the uncomplicated voltammogram confirmed electrochemical purity of our synthesized compounds [63].

3. Pharmacology

Screening of synthesized substances and cisplatin used as reference was carried out using lung cancer A549, H322 and H1299 cell lines. Proliferation percentage was determined by the sulforhodamine B (SRB) assay. Cells were incubated with substances at 20, 40 and 60 μM for 48 h and the cell proliferation/viability determination using the survival percentage obtained with the cell treated only with the solvent (DMSO at 0.1%) as reference. The results are expressed as the average of triplicate assays.

4. Results and discussion

4.1. Effects of the compounds on the viability of A549 lung cancer cells

In order to evaluate the inhibitory effects of the compounds on growth of A549 cells we carried out the SRB assay with the compounds at the concentration of 40 μM for 48 h. These compounds are stable in the media used for biological evaluation during the time of testing. The results showed that the compounds (*S*)- and (*R*)-**2b**–**d** displayed great effects on the growth of the cells as shown in Fig. 4. Although the effects of these compounds are inferior to cisplatin, it is interesting that the compounds substituted with –OMe and –F persistently show different behavior than the –H one. The reason might be in electronic and steric characteristics of compounds as well as hydrophilic–hydrophobic balance of the molecules. Furthermore, in order to compare the different biological properties of the compounds with and without ferrocene, we performed the anti-cancer activity evaluation of them. We can see from Fig. 4 that the effects of compounds (*S*)- and (*R*)-**2b** with ferrocene on the growth of the cells excel that one of the compounds (*R*)-**5** and (*S*)-**5** without ferrocene. Moreover, the starting materials, compounds (*R*)-**1** and (*S*)-**1**, have only weak effects on the growth of A549 cells.

Furthermore, Fig. 5 indicates the cytotoxic effects of the compounds tested at different concentration on the viability of A549, H322 and H1299 lung cancer cells that were incubated for 48 h. The viability of 3 cell lines was significantly dose-dependently suppressed by these compounds. Growth inhibitory properties (IC_{50},

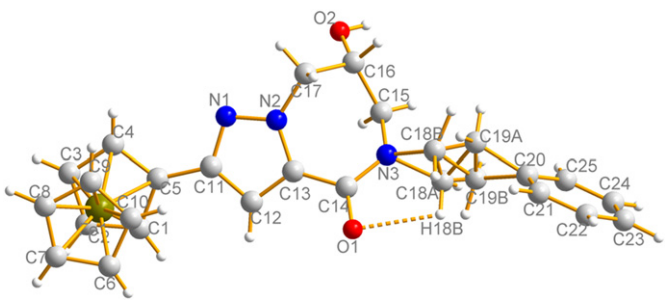

Fig. 1. X-ray crystal structure of compound (*R*)-**2a**. The C–H···O intramolecular hydrogen bond is shown with orange dashed line.(For interpretation of the references to colour in this figure legend, the reader is referred to the web version of this article.)

Table 2
Summary of crystal data and structure refinement.

Compound	(*R*)-**2a**
Empirical formula	$C_{25}H_{25}FFeN_3O_2$
Formula weight	455.33
Crystal system	Triclinic
Space group	P-1
a (Å)	7.6782(7)
b (Å)	10.4352(9)
c (Å)	13.2430(12)
α (°)	87.263(2)
β (°)	87.660(2)
γ (°)	86.4970(10)
Z	2
Calculated density [Mg/m^3]	1.430
Crystal size [mm]	0.08 × 0.1 × 0.1
Absorption coefficient [mm^{-1}]	0.741
F (000)	476
Reflection collected	3554
Data/restraints/parameters	2194/54/362
θ Range for data collection [°]	1.54–20.79
Ranges of indices *h*, *k*, *l*	$-7 \le h \le 6$, $-10 \le k \le 9$, $-13 \le l \le 9$
Final *R* indices [$I > 2\sigma(I)$]	$R_1 = 0.0459$, $\omega R_2 = 0.1148$
R indices (all data)	$R_1 = 0.0554$, $\omega R_2 = 0.1227$
Goodness of fit on F^2	1.026
$\Delta\rho$ (max/min) [e Å^{-3}]	0.748; −0.351

Table 3
Selected bond lengths [Å] and angles [°] for Compound (*R*)-**2a**.

Fe(1)–C(10)	2.021(7)
Fe(1)–C(9)	2.020(7)
Fe(1)–C(8)	2.033(7)
Fe(1)–C(7)	2.025(6)
Fe(1)–C(6)	2.025(6)
Fe(1)–C(5)	2.040(5)
Fe(1)–C(4)	2.027(5)
Fe(1)–C(3)	2.030(5)
Fe(1)–C(2)	2.034(5)
Fe(1)–C(1)	2.033(6)
O(2)–C(16)	1.365(7)
O(1)–C(14)	1.242(6)
C(15)–N(3)–C(14)	121.1(5)
C(17)–N(2)–C(13)	126.9(5)
N(1)–N(2)–C(17)	121.0(5)
N(1)–N(2)–C(13)	111.9(4)
N(2)–N(1)–C(11)	104.7(4)
N(2)–C(17)–C(16)	113.8(6)
O(2)–C(16)–C(17)	109.0(6)
O(2)–C(16)–C(15)	112.6(6)
C(17)–C(16)–C(15)	112.1(6)
N(3)–C(15)	1.470(8)
N(3)–C(14)	1.339(7)
N(2)–N(1)	1.346(5)
N(2)–C(17)	1.453(7)
N(2)–C(13)	1.360(6)
N(1)–C(11)	1.345(6)
C(17)–C(16)	1.495(9)
C(16)–C(15)	1.518(11)
C(14)–C(13)	1.473(7)
C(13)–C(12)	1.365(7)
C(12)–C(11)	1.387(7)
C(11)–C(5)	1.464(7)
N(3)–C(15)–C(16)	117.5(7)
O(1)–C(14)–N(3)	122.2(5)
O(1)–C(14)–C(13)	119.7(5)
N(3)–C(14)–C(13)	118.2(5)
N(2)–C(13)–C(14)	123.8(5)
N(2)–C(13)–C(12)	106.6(4)
C(13)–C(12)–C(11)	105.8(5)
N(1)–C(11)–C(12)	111.0(4)

μM) of the compounds and cisplatin at 48 h in A549, H322 and H1299 cell were shown in Table 6. The results indicated that these compounds had selective effects on the proliferation of A549, H322 and H1299 cells, though their inhibitory effects are inferior to cisplatin. The compounds possessed more effective inhibition for A549 than other cell lines. Among them, (*R*)-**2b** with methoxy group in 3-position of benzene moiety showed the most potent inhibitory effect on A549 cells growth. However, (*S*)-**2d** with fluorine group in 2-position of benzene moiety displayed a most potent growth inhibition for H322 and H1299 cells. The results showed that the anti-tumor activities of these compounds were related to the nature of substituents in benzene moiety. Moreover, (*R*)-**2b** possessed more effective inhibition than (*S*)-**2b**, for which their IC_{50} are 27.5 and 38.9 for A549 cell, meanwhile (*S*)-**2d** showed more effective inhibition than (*R*)-**2d**, for which their IC_{50} are 43.8 and 53.9 for H322 cell, respectively. But, the inhibition differences between *R* and *S* enantiomers are mostly not so significant, so the chirality of the synthesized compounds almost doesn't have any influence in the inhibition on the tested cancer cells. The results indicated also that compounds **2b**–**d** possessed notable cytotoxicity and selectivity for A549 vs H1299 and H322 lung cancer cells.

Table 4
Hydrogen-bond geometry for (*R*)-**2a**.

X–H···A/π[a]	X–H	H···A/π	X···A/π	X–H···A/π	Symmetry codes
O2–$H2_A$···O1	0.82	2.13	2.860(6)	148	$1 + x, y, z$
$C18_A$–$H18_B$···O1	0.96	2.28	2.704(10)	106	
C17–$H17_A$···Cg3		2.70(6)	3.551(8)	157(5)	$-x, 1 - y, -z$
$C19_A$–$H19_A$···Cg4		2.68	3.274(10)	121	$1 - x, -y, 1 - z$

[a] Cg3 and Cg4 are the centroids of the cyclopentadienyl ring and the benzene ring, respectively.

4.2. Compounds induced apoptosis in H322 and H1299 cells

The mode of cell killing induced by most anti-cancer agents is apoptotic cell death. To detect whether selected compounds result in apoptosis of the cells, we performed Hoechst 33258 staining assay. It is well known that DNA fragmentation, chromatin condensation, cell shrinkage, and membrane blebbing are the characteristics of apoptotic cells. The chromatin condensation and DNA fragmentation in the cells were determined by Hoechst 33258 staining under a fluorescence microscope. It was observed that compounds (*S*)- and (*R*)-**2b**–**d** at the concentration of 40 μM for 48 h induced apoptosis in H322 cells greatly ($p < 0.05$ vs control, Fig. 6). The compounds (*S*)- and (*R*)-**2b**–**d** at the concentration of 60 μM for 48 h induced apoptosis in H1299 cells greatly ($p < 0.05$ vs control, Fig. 7). However, the compounds tested did not induce apoptosis in A549 cells (data not shown).

4.3. Flow cytometry analysis of cell cycle distribution

The eukaryotic cell cycle consists of alternating rounds of DNA replication (S phase) and cell division (M phase) separated by the gap phases G0–G2. It is known that regulation of proteins to mediate critical events in the cell cycle may be a useful anti-tumor strategy [64]. Thus, what we need to know is whether the selected compounds induce A549 cell cycle arrest. The results of cytometry analysis showed that tested compounds treatment with 40 μM at 48 h induced G1-phase arrest effectively as shown in Fig. 8 which is one representative experiment from three independent experiments. After 48 h treatment with 40 μM compounds tested, the G1 population was noticeably enhanced by 21–34% compared with control. The increase in the G1-phase cell population was accompanied by a decrease in the S and G2-phase cell populations. The strong G1-phase arrest induced by tested compounds is concomitant with the growth inhibitory effect.

The compounds might perform their action through inducing a strong G1-phase arrest rather than apoptosis for A549 cell, whereas by inducing apoptosis for H322 and H1299 cells.

4.4. Necrosis detection by LDH activity assay

In order to determine if the growth inhibitory effects were due to necrosis that is believed to be an unwanted side effect of cancer-fighting agents, LDH assay was performed on cells treated with compounds (*S*)- and (*R*)-**2b**–**d** or 0.1% DMSO (as control). As shown in Fig. 9, there were no significant differences in LDH release between the cells in the control group and the compounds treatment groups. The results indicated that the compounds at the test range of concentration did not cause necrosis in the cells.

5. Conclusion

We have described a facile approach to prepare 2-ferrocenyl-7-hydroxy-5-phenethyl-5,6,7,8-tetrahydro-4*H*-pyrazolo[1,5-a][1,4]diazepin-4-one derivatives with optical activity by the reaction of substituted phenylethylamine and ethyl 3-ferrocenyl-1-(oxiran-2-ylmethyl)-1*H*-pyrazole-5-carboxylate under the general heating condition and the microwave-assisted condition. Microwave-assisted reaction in solvent-free is fast 50 fold than general heating method in sealed tube. A representative single-

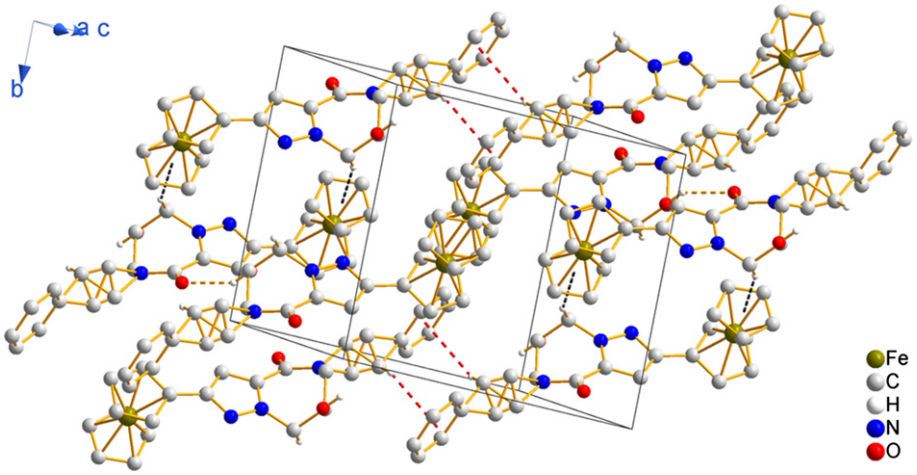

Fig. 2. Packing diagram of (*R*)-**2a**. Hydrogen bonds and C–H···π interactions are shown with orange, red and black dashed lines.(For interpretation of the references to colour in this figure legend, the reader is referred to the web version of this article.)

crystal structural characterization of the compound (*R*)-**2a** by X-ray is valuable for further investigation. Although (*R*)-**2b** displayed more effective inhibition than (*S*)-**2b** for A549 cells, and (*S*)-**2d** was more effect than (*R*)-**2d** for H322 cells, the inhibition differences between *R* and *S* enantiomers are mostly not so significant. So for the compounds synthesized, chirality almost doesn't have any influence in the inhibition on the tested cancer cells. The anti-tumor activities of these compounds were related to the nature of substituents in benzene moiety and the compounds substituted with –OMe or –F were more effective than the –H one. The compounds **2b**–**d** possessed notable cytotoxicity and selectivity for A549 vs H1299 and H322 lung cancer cells due to the compounds could inhibit growth of A549, H322 and H1299 cells in different mechanism. Compounds (*S*)- and (*R*)-**2a**–**d** inhibited growth of A549 cells by inducing a strong G1-phase arrest. Whereas these compounds inhibited growth of H1299 and H322 cells by inducing apoptosis.

6. Experimental

6.1. General

Analytical TLC was performed on silica gel 60 F_{254} plates (Merck KGaA). Melting points were determined on an XD-4 digital micromelting point apparatus. ^{1}H NMR spectra were recorded on a Bruker Avance 300 (300 MHz) spectrometer, using DMSO as solvent and tetramethylsilane (TMS) as internal standard. IR spectra were recorded with an IR spectrophotometer Avtar 370 FT-IR (Thermo Nicolet). Electrospray ionization mass spectrometry (ESI-MS) spectra were recorded on a LTQ Orbitrap Hybrid mass spectrograph. All microwave-assisted reactions were carried out in a START SYNTH Microwave Synthesis Lab station. Cyclic voltammetry measurements were performed on a CHI760C electrochemical workstation (Shanghai China) using a three-electrode cell equipped with a glassy carbon (GC) electrode ($A = 0.2$ cm^2) as the working electrode, a platinum sheet with a surface of 4 cm^2 served as the counter electrode, and a saturated calomel electrode (SCE) as the reference electrode. The CH_2Cl_2 for electrochemical use was distilled from CaH_2 and deoxygenated by saturation with N_2.

Table 5
Electrochemical data for compounds (*R*)- and (*S*)-**2a**–**d** obtained at a scan rate of 0.2 V/s at RT in CH_2Cl_2/Bu_4NPF_6 (0.1 M) as the supporting electrolyte.

Compound	(*S*)-**2a**	(*S*)-**2b**	(*S*)-**2c**	(*S*)-**2d**	(*R*)-**2a**	(*R*)-**2b**	(*R*)-**2c**	(*R*)-**2d**
$E^{0'}$ [V][a]	0.451	0.453	0.452	0.459	0.456	0.455	0.456	0.454

[a] $E^{0'} = (E_{pa} + E_{pc})/2$.

6.2. General procedure for the synthesis of 5-arylethyl-2-ferrocenyl-7-hydroxy-5,6,7,8-tetrahydro-4H-pyrazolo[1,5-a][1,4]diazepin-4-one **2** [(*S*)-**2** and (*R*)-**2**] by classical heating technique

The mixture of ethyl 3-ferrocenyl-1-(oxiran-2-ylmethyl)-1*H*-pyrazole-5-carboxylate **1** (3 mmol) and the corresponding 2-arylethanamine (3.6 mmol) in absolute alcohol (50 mL) was stirred and heated at reflux for 10 h under N_2. Then the reaction mixture was cooled to room temperature and concentrated under reduced pressure. The residue was purified by column chromatography on silica gel with the eluent system of ethyl acetate/petroleum ether ($v/v = 1{:}1$) to afford the product **2** in 20–28% yield.

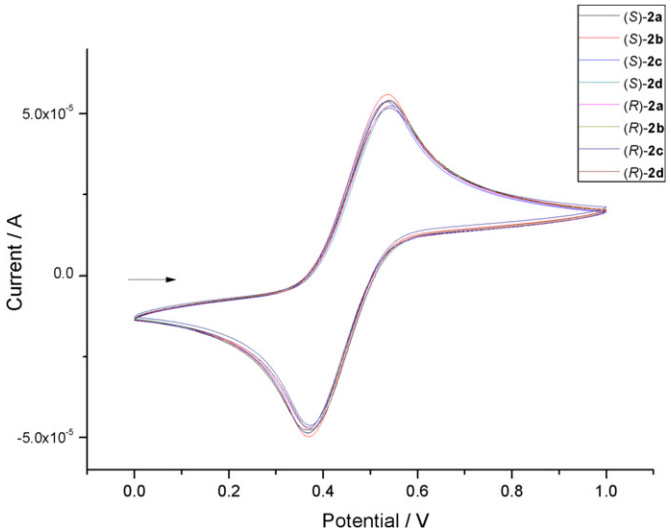

Fig. 3. Cyclic voltammograms of (*S*)- and (*R*)-**2a**-**d** in CH_2Cl_2/NBu_4PF_6 (0.1 M) at a scan rate of 0.2 V/s at RT.

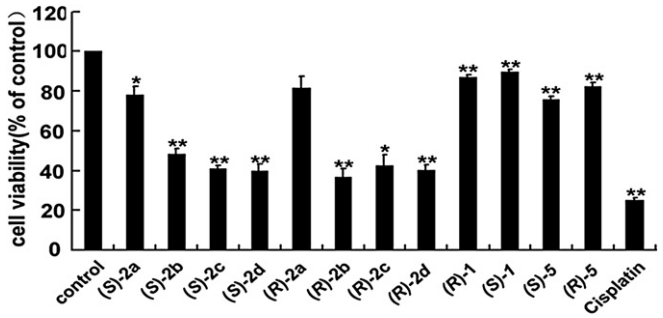

Fig. 4. Effects of the compounds on A549 cell viability. A549 cells were treated with compounds (*S*)- and (*R*)-**2a**–**d**, (*S*)- and (*R*)-**1**, (*S*)- and (*R*)-**5**, cisplatin or 0.1% DMSO (control) for 48 h at the concentration of 40 μM.

6.3. General procedure for the synthesis of 5-arylethyl-2-ferrocenyl-7-hydroxy-5,6,7,8-tetrahydro-4H-pyrazolo[1,5-a][1,4]diazepin-4-one **2** [(S)-**2** and (R)-**2**] in sealed tube

The solution of compound **1** (0.5 mmol) and the corresponding 2-arylethanamine (0.6 mmol) in absolute alcohol (10 mL) was stirred in a sealed tube and heated in an oil bath at 140 °C for 8–12 h. Then the reaction mixture was cooled to room temperature and concentrated under reduced pressure. The residue was purified by column chromatography on silica gel with the eluent system of ethyl acetate/petroleum ether (*v*/*v* = 1:1) to afford the product **2** in 62–82% yield.

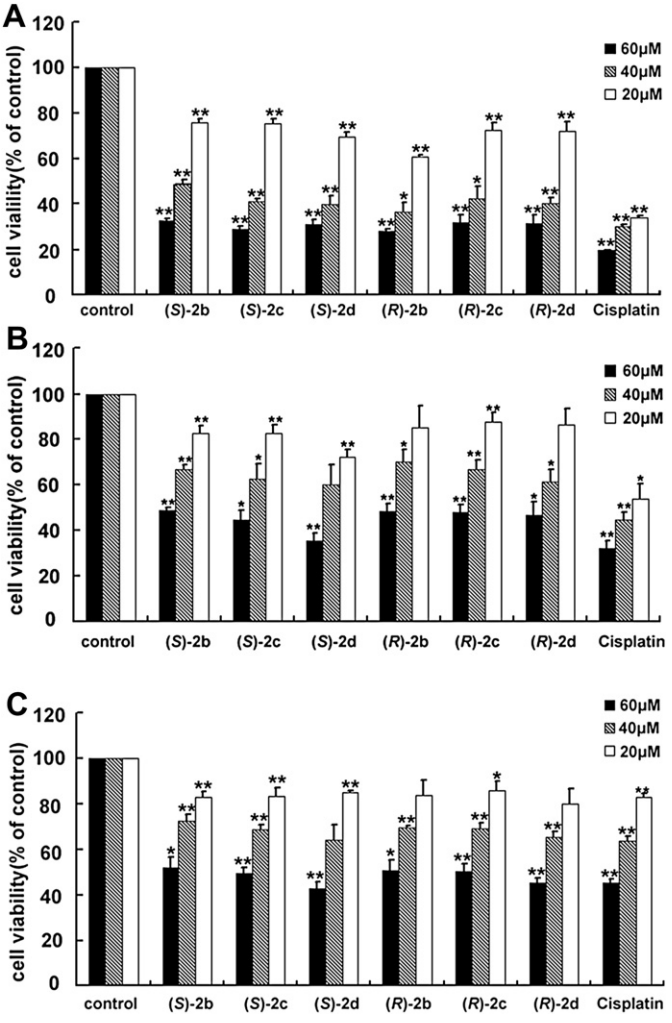

Fig. 5. Effects of the compounds on A549, H322 and H1299 cell viability. Cells were treated with compounds (*S*)- and (*R*)-**2b**–**d** and cisplatin (reference) or 0.1% DMSO (control) for 48 h at the concentration of 20, 40 or 60 μM respectively. A: A549; B: H322; C: H1299. Cell viability was analyzed by SRB assay. Data are mean ± SD from three independent experiments (*, $p < 0.05$ and **, $p < 0.01$ vs control).

Table 6
Growth inhibitory properties for the compounds at 48 h in A549, H322 and H1299 lung cancer cells.

Compounds	IC_{50} (μM) ± SD		
	A549	H322	H1299
(*S*)-**2b**	38.9 ± 4.05	60.8 ± 3.22	70.6 ± 5.59
(*S*)-**2c**	35.4 ± 2.50	53.6 ± 12.1	62.7 ± 3.73
(*S*)-**2d**	33.2 ± 6.68	43.8 ± 15.6	52.3 ± 11.9
(*R*)-**2b**	27.5 ± 7.29	61.5 ± 9.53	65.3 ± 1.43
(*R*)-**2c**	35.6 ± 9.37	57.7 ± 6.91	62.7 ± 4.36
(*R*)-**2d**	34.6 ± 4.33	53.9 ± 10.0	56.4 ± 4.16
(*S*)-**1**	96.9 ± 0.04	–	–
(*R*)-**1**	135.7 ± 0.03	–	–
(*S*)-**5**	118.9 ± 0.02	–	–
(*S*)-**5**	100.5 ± 0.03	–	–
Cisplatin	14.79 ± 0.45	21.15 ± 0.69	45.42 ± 1.67

Data are shown as the mean values of three independent experiments with the corresponding standard deviation (SD), "–" not determined.

6.4. General procedure for the synthesis of 5-arylethyl-2-ferrocenyl-7-hydroxy-5,6,7,8-tetrahydro-4H-pyrazolo[1,5-a][1,4]diazepin-4-one **2** [(S)-**2** and (R)-**2**] by microwave-assisted technique

To a glass vessel, compound **1** (0.5 mmol) and the corresponding 2-arylethanamine (0.6 mmol) was added and then irradiated in the microwave cavity, keeping the reaction temperature at 70 °C for 10–15 min. Then the reaction mixture was cooled to room temperature and purified by column chromatography on silica gel with the eluent system of ethyl acetate/petroleum ether (*v*/*v* = 1:1) to afford the product **2** in 72–81% yield.

6.4.1. (S)-2-ferrocenyl-7-hydroxy-5-phenethyl-5,6,7,8-tetrahydro-4H-pyrazolo[1,5-a][1,4]diazepin-4-one [(S)-**2a**]

Yellow solid, mp 218–220 °C, $[\alpha]_D^{30} = +20.2$ ($c = 0.4$, $CHCl_3$). IR (KBr), ν/cm^{-1}: 3425 (O–H), 2941, 2869 (C–H), 1609 (C=O), 1526 (C=N), 1454, 1269, 1177, 810, 756, 506, 485 (CpFeCp). ^1H NMR: δ 2.92 (t, $J = 7.5$ Hz, 2H, CH_2), 3.06 (dd, $J = 14.8$ Hz, 7.0 Hz, 1H, CH_2), 3.38 (dd, $J = 14.8$ Hz, 4.6 Hz, 1H, CH_2), 3.58 (dt, $J = 13.5$ Hz, 7.5 Hz, 1H, CH_2), 3.87 (dt, $J = 13.5$ Hz, 7.5 Hz, 1H, CH_2), 4.04 (s, 5H, C_5H_5), 4.07 (dd, $J = 12.0$ Hz, 3.8 Hz, 1H, CH_2), 4.20–4.30 (m, 2H, CH_2, CH), 4.27 (t, $J = 1.8$ Hz, 2H, C_5H_4), 4.70 (t, $J = 1.8$ Hz, 2H, C_5H_4), 5.47 (d, $J = 3.9$ Hz, 1H, OH), 6.82 (s, 1H, 4-H), 7.20–7.35 (m, 5H, ArH). HRMS calcd for $C_{25}H_{26}FeN_3O_2$ $[M + H]^+$: 456.1374, found: 456.1363.

6.4.2. (S)-2-ferrocenyl-7-hydroxy-5-(3-methoxyphenethyl)-5,6,7,8-tetrahydro-4H-pyrazolo[1,5-a][1,4]diazepin-4-one [(S)-**2b**]

Yellow solid, mp 155–158 °C, $[\alpha]_D^{30} = +21.9$ ($c = 0.4$, $CHCl_3$). IR (KBr), ν/cm^{-1}: 3440 (O–H), 2923, 2832 (C–H), 1643 (C=O), 1522 (C=N), 1455, 1481, 1258, 998, 786, 507, 482 (CpFeCp). ^1H NMR: δ 2.89 (t, $J = 7.5$ Hz, 2H, CH_2), 3.05 (dd, $J = 15.0$ Hz, 6.9 Hz, 1H, CH_2), 3.38 (dd, $J = 15.0$ Hz, 4.8 Hz, 1H, CH_2), 3.57 (dt, $J = 13.5$ Hz, 7.5 Hz, 1H, CH_2), 3.75 (s, 3H, CH_3), 3.86 (dt, $J = 13.5$ Hz, 7.5 Hz, 1H, CH_2), 4.04 (s, 5H, C_5H_5), 4.02–4.10 (m, 1H, CH_2), 4.20–4.33 (m, 2H, CH_2, CH), 4.28 (t, $J = 1.8$ Hz, 2H, C_5H_4), 4.70 (t, $J = 1.8$ Hz, 2H, C_5H_4), 5.48 (d, $J = 3.9$ Hz, 1H, OH), 6.78–6.87 (m, 3H, ArH), 6.82 (s, 1H, 4-H), 7.23 (t, $J = 8.1$ Hz, 1H, ArH). HRMS calcd for $C_{26}H_{28}FeN_3O_3$ $[M + H]^+$: 486.1480, found: 486.1485.

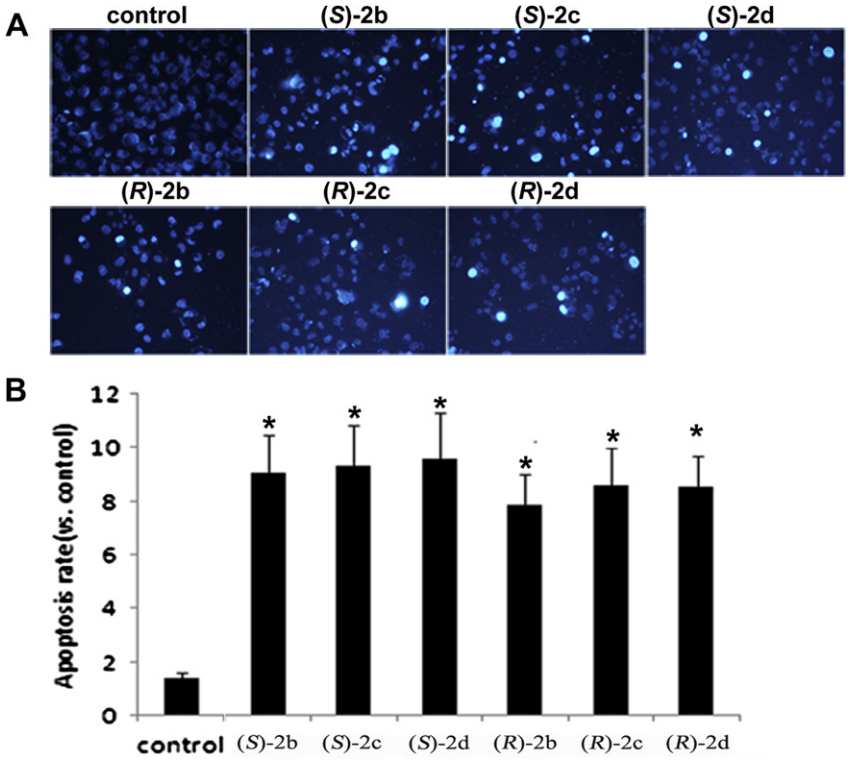

Fig. 6. Compounds induced H322 cell apoptosis significantly. A: Fluorescent micrographs of Hoechst 33258 staining (200×). The cells were treated with DMSO 0.1% (*v*/*v*) as a vehicle control and were treated with the compounds (*S*)- and (*R*)-**2b**–**d** at concentrations of 40 μM respectively; B: Ratio of apoptotic cells vs control. Results are presented as mean ± SD; ($n = 3$. *, $p < 0.05$ vs control).

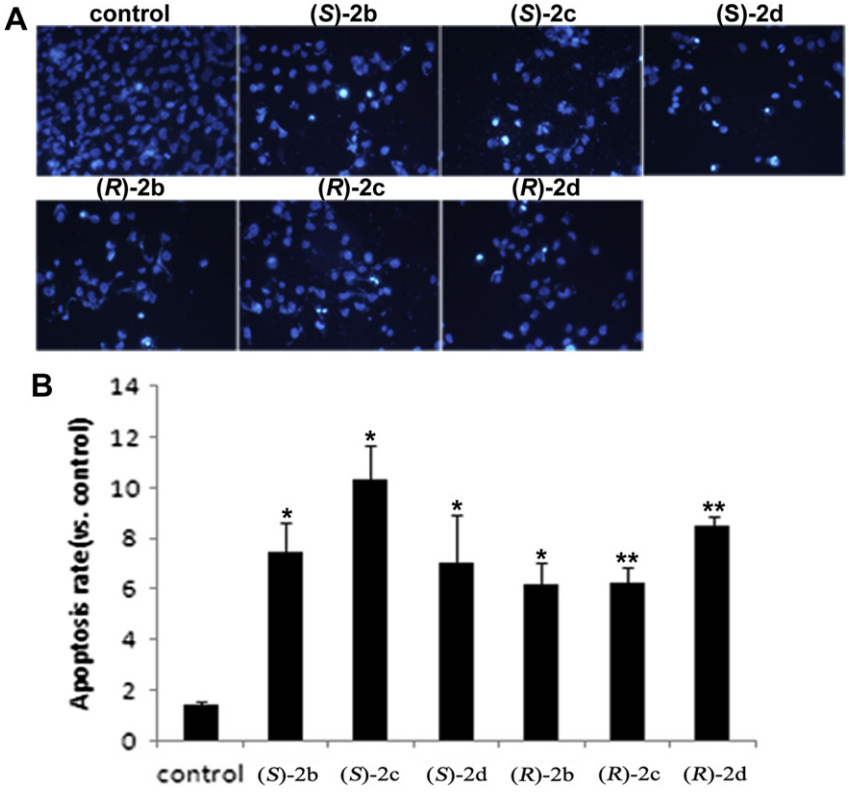

Fig. 7. Compounds induced H1299 cell apoptosis significantly. A: Fluorescent micrographs of Hoechst 33258 staining (200×). The cells were treated with DMSO 0.1% (*v*/*v*) as a vehicle control and were treated with the compounds (*S*)- and (*R*)-**2b**–**d** at concentrations of 60 μM respectively. B: Ratio of apoptotic cells vs control. Results are presented as mean ± SD; ($n = 3$. *, $p < 0.05$ vs control; **, $p < 0.01$ vs control).

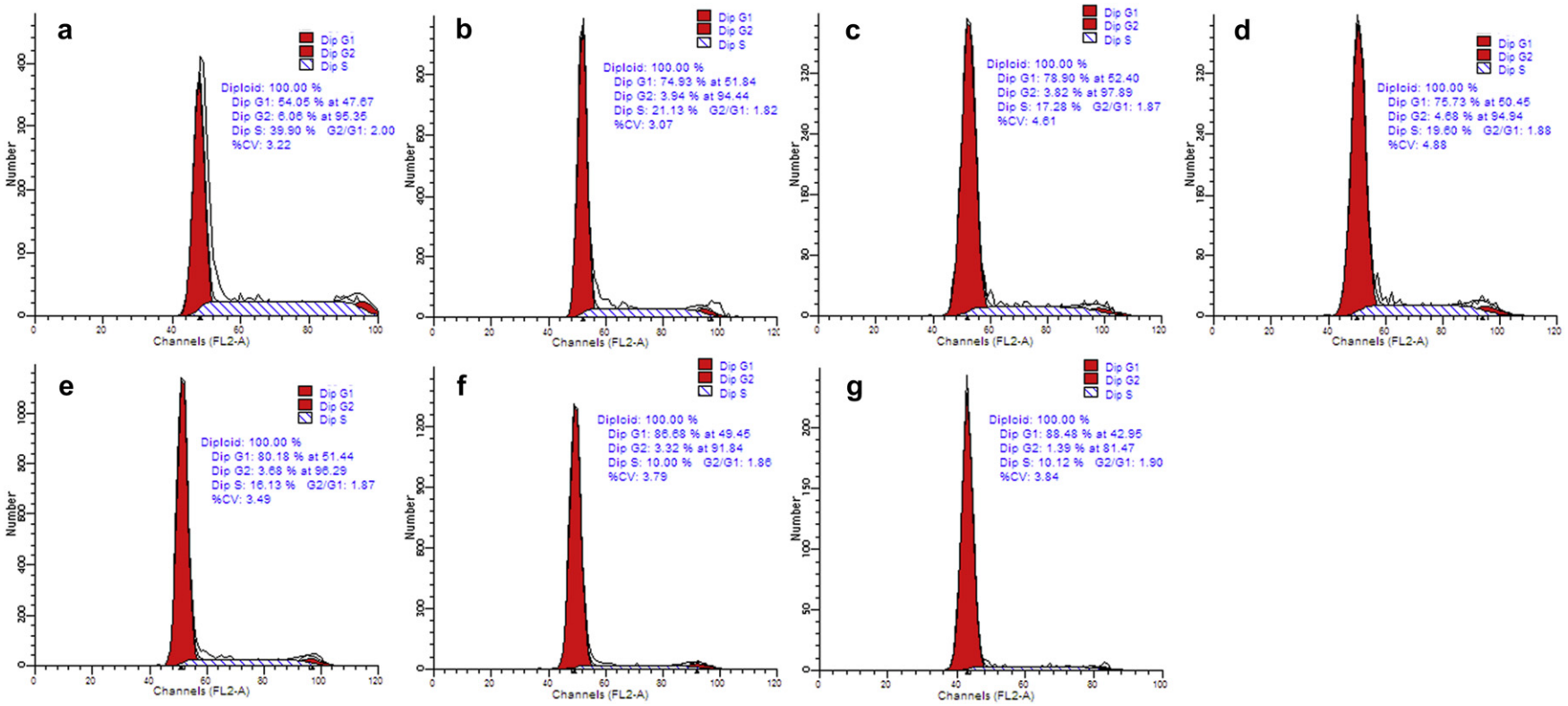

Fig. 8. Effect of compounds (*S*)- and (*R*)-**2b**–**d** on cell cycle distribution of A549 lung cancer cells. Cells were exposed to the compounds at 40 μM and incubated for 48 h, and then were stained with PI. Values are expressed as percentage of the cell population in the G1, S, and G2 phase of cell cycle. A: Control; B: (*S*)-**2b**; C: (*S*)-**2c**; D: (*S*)-**2d**; E: (*R*)-**2b**; F: (*R*)-**2c**; G: (*R*)-**2d**.

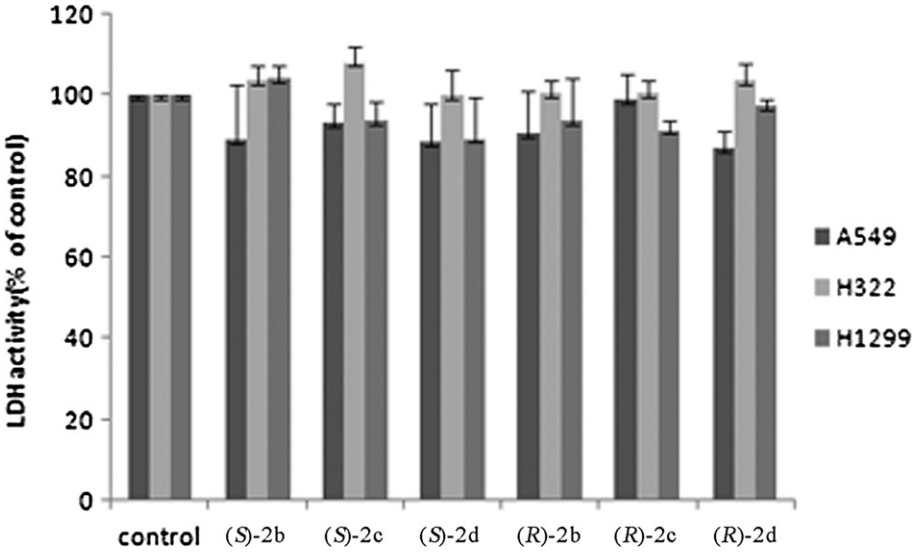

Fig. 9. Effects of the compounds on LDH release in A549, H322 and H1299 cells. The cells were treated with compounds (*S*)- and (*R*)-**2b**–**d** at concentrations of 40 μM or left untreated (control) for 48 h. LDH assay results are presented as mean ± SD; $n = 3$.

*6.4.3. (S)-2-ferrocenyl-5-(4-fluorophenethyl)-7-hydroxy-5,6,7,8-tetrahydro-4H-pyrazolo[1,5-a][1,4]diazepin-4-one [(S)-**2c**]*

Yellow solid, mp 162–165 °C, $[\alpha]_D^{30} = +15.6$ ($c = 0.4$, $CHCl_3$). IR (KBr), ν/cm^{-1}: 3342 (O–H), 3098, 2936 (C–H), 1613 (C=O), 1529 (C=N), 1507, 1364, 1218, 815, 503, 486 (CpFeCp). ^{1}H NMR: δ 2.91 (t, $J = 7.5$ Hz, 2H, CH_2), 3.07 (dd, $J = 15.0$ Hz, 4.2 Hz, 1H, CH_2), 3.39 (dd, $J = 15.0$ Hz, 5.1 Hz, 1H, CH_2), 3.57 (dt, $J = 13.2$ Hz, 7.5 Hz, 1H, CH_2), 3.83 (dt, $J = 13.2$ Hz, 7.5 Hz, 1H, CH_2), 4.04 (s, 5H, C_5H_5), 4.07 (dd, $J = 14.1$ Hz, 3.9 Hz, 1H, CH_2), 4.17–4.20 (m, 1H, CH), 4.27 (t, $J = 1.8$ Hz, 2H, C_5H_4), 4.29 (dd, $J = 14.1$ Hz, 5.4 Hz, 1H, CH_2), 4.69 (t, $J = 1.8$ Hz, 2H, C_5H_4), 6.81 (s, 1H, 4-H), 5.49 (d, $J = 3.9$ Hz, 1H, OH), 7.14 (t, $J = 8.9$ Hz, 2H, ArH), 7.33 (t, $J = 7.1$ Hz, 2H, ArH). HRMS calcd for $C_{25}H_{25}FFeN_3O_2$ $[M + H]^+$: 474.1280, found: 474.1286.

*6.4.4. (S)-5-(2-fluorophenethyl)-7-hydroxy-2-ferrocenyl-5,6,7,8-tetrahydro-4H-pyrazolo[1,5-a][1,4]diazepin-4-one [(S)-**2d**]*

Yellow solid, mp 177–178 °C, $[\alpha]_D^{30} = +15.0$ ($c = 0.4$, $CHCl_3$). IR (KBr), ν/cm^{-1}: 3402 (O–H), 3085, 2949, 2866 (C–H), 1621 (C=O), 1532 (C=N), 1461, 1420, 1104, 758, 510, 486 (CpFeCp). ^{1}H NMR: δ 2.96 (t, $J = 7.5$ Hz, 2H, CH_2), 3.08 (dd, $J = 15.0$ Hz, 6.9 Hz, 1H, CH_2), 3.37 (dd, $J = 15.0$ Hz, 5.1 Hz, 1H, CH_2), 3.61 (dt, $J = 13.2$ Hz, 7.5 Hz, 1H, CH_2), 3.82 (dt, $J = 13.2$ Hz, 7.5 Hz, 1H, CH_2), 4.04 (s, 5H, C_5H_5), 4.08 (dd, $J = 14.1$ Hz, 4.2 Hz, 1H, CH_2), 4.20–4.27 (m, 1H, CH), 4.28 (t, $J = 1.8$ Hz, 2H, C_5H_4), 4.30 (dd, $J = 14.1$ Hz, 5.4 Hz, 1H, CH_2), 4.70 (t, $J = 1.8$ Hz, 2H, C_5H_4), 5.51 (d, $J = 4.2$ Hz, 1H, OH), 6.81 (s, 1H, 4-H), 7.15(d, $J = 7.2$ Hz, 1H, ArH), 7.19 (d, $J = 8.1$ Hz, 1H, ArH), 7.29 (t, $J = 7.2$ Hz, 1H, ArH), 7.38 (t, $J = 7.5$ Hz, 1H, ArH). HRMS calcd for $C_{25}H_{25}FFeN_3O_2$ $[M + H]^+$: 474.1280, found: 474.1283.

*6.4.5. (R)-2-ferrocenyl-7-hydroxy-5-phenethyl-5,6,7,8-tetrahydro-4H-pyrazolo[1,5-a][1,4]diazepin-4-one [(R)-**2a**]*

Yellow solid, mp 219–220 °C, $[\alpha]_D^{30} = -20.4$ ($c = 0.4$, $CHCl_3$). IR (KBr), ν/cm^{-1}: 3398 (O–H), 2923, 2869 (C–H), 1607 (C=O), 1526 (C=N), 1454, 1266, 1177, 810, 756, 506, 484 (CpFeCp). ^{1}H NMR: δ 2.92 (t, $J = 7.5$ Hz, 2H, CH_2), 3.06 (dd, $J = 15.0$ Hz, 7.0 Hz, 1H, CH_2), 3.38 (dd, $J = 14.8$ Hz, 4.8 Hz, 1H, CH_2), 3.58 (dt, $J = 13.5$ Hz, 7.5 Hz, 1H, CH_2), 3.86 (dt, $J = 13.5$ Hz, 7.5 Hz, 1H, CH_2), 4.04 (s, 5H, C_5H_5), 4.07 (dd, $J = 12.0$ Hz, 3.6 Hz, 1H, CH_2), 4.19–4.30 (m, 2H, CH_2, CH), 4.27 (t, $J = 1.8$ Hz, 2H, C_5H_4), 4.70 (t, $J = 1.8$ Hz, 2H, C_5H_4), 5.47 (d, $J = 3.9$ Hz, 1H, OH), 6.82 (s, 1H, 4-H), 7.20–7.35 (m, 5H, ArH); ^{13}C NMR (DMSO, 75 MHz): δ 161.6, 148.5, 138.9, 138.5, 128.7(2C), 128.4(2C), 126.2, 105.8, 78.0, 69.4, 69.2(5C), 68.2(2C), 66.2, 66.1, 55.3, 52.7, 49.2, 33.7. HRMS calcd for $C_{25}H_{26}FeN_3O_2$ $[M + H]^+$: 456.1374, found: 456.1375.

*6.4.6. (R)-2-ferrocenyl-7-hydroxy-5-(3-methoxyphenethyl)-5,6,7,8-tetrahydro-4H-pyrazolo[1,5-a][1,4]diazepin-4-one [(R)-**2b**]*

Yellow solid, mp 158–160 °C, $[\alpha]_D^{30} = -22.3$ ($c = 0.4$, $CHCl_3$). IR (KBr), ν/cm^{-1}: 3420 (O–H), 3097, 2927, 2869 (C–H), 1644 (C=O), 1526 (C=N), 1457, 1258, 1161, 1029, 787, 508, 483 (CpFeCp). ^{1}H NMR: δ 2.89 (t, $J = 7.5$ Hz, 2H, CH_2), 3.05 (dd, $J = 15.0$ Hz, 6.9 Hz, 1H, CH_2), 3.38 (dd, $J = 15.0$ Hz, 4.8 Hz, 1H, CH_2), 3.57 (dt, $J = 13.5$ Hz, 7.5 Hz, 1H, CH_2), 3.75 (s, 3H, CH_3), 3.86 (dt, $J = 13.5$ Hz, 7.5 Hz, 1H, CH_2), 4.04 (s, 5H, C_5H_5), 4.02–4.10 (m, 1H, CH_2), 4.20–4.33 (m, 2H, CH_2, CH), 4.28 (t, $J = 1.8$ Hz, 2H, C_5H_4), 4.70 (t, $J = 1.8$ Hz, 2H, C_5H_4), 5.47 (d, $J = 3.9$ Hz, 1H, OH), 6.78–6.87 (m, 3H, ArH), 6.82 (s, 1H, 4-H), 7.23 (t, $J = 8.1$ Hz, 1H, ArH). HRMS calcd for $C_{26}H_{28}FeN_3O_3$ $[M + H]^+$: 486.1480, found: 486.1468.

*6.4.7. (R)-2-ferrocenyl-5-(4-fluorophenethyl)-7-hydroxy-5,6,7,8-tetrahydro-4H-pyrazolo[1,5-a][1,4]diazepin-4-one [(R)-**2c**]*

Yellow solid, mp 172–175 °C, $[\alpha]_D^{30} = -14.2$ ($c = 0.4$, $CHCl_3$). IR (KBr), ν/cm^{-1}: 3348 (O–H), 3098, 2936 (C–H), 1613 (C=O), 1530 (C=N), 1408, 1365, 1217, 817, 503, 486 (CpFeCp). ^{1}H NMR: δ 2.91 (t, $J = 7.5$ Hz, 2H, CH_2), 3.07 (dd, $J = 15.0$ Hz, 4.2 Hz, 1H, CH_2), 3.39 (dd, $J = 15.0$ Hz, 5.1 Hz, 1H, CH_2), 3.57 (dt, $J = 13.2$ Hz, 7.5 Hz, 1H, CH_2), 3.83 (dt, $J = 13.2$ Hz, 7.5 Hz, 1H, CH_2), 4.04 (s, 5H, C_5H_5), 4.07 (dd, $J = 13.8$ Hz, 3.9 Hz, 1H, CH_2), 4.17–4.20 (m, 1H, CH), 4.27 (t, $J = 1.8$ Hz, 2H, C_5H_4), 4.29 (dd, $J = 14.1$ Hz, 5.4 Hz, 1H, CH_2), 4.69 (t, $J = 1.8$ Hz, 2H, C_5H_4), 6.81 (s, 1H, 4-H), 5.48 (d, $J = 3.9$ Hz, 1H, OH), 7.14 (t, $J = 8.9$ Hz, 2H, ArH), 7.33 (t, $J = 7.1$ Hz, 2H, ArH). HRMS calcd for $C_{25}H_{25}FFeN_3O_2$ $[M + H]^+$: 474.1280, found: 474.1263.

*6.4.8. (R)-2-ferrocenyl-5-(2-fluorophenethyl)-7-hydroxy-5,6,7,8-tetrahydro-4H-pyrazolo[1,5-a][1,4]diazepin-4-one [(R)-**2d**]*

Yellow solid, mp 180–183 °C, $[\alpha]_D^{30} = -15.6$ ($c = 0.4$, $CHCl_3$). IR (KBr), ν/cm^{-1}: 3401 (O–H), 3086, 2944, 2870 (C–H), 1613 (C=O), 1529 (C=N), 1456, 1232, 1102, 757, 508, 486 (CpFeCp). ^{1}H NMR: δ 2.96 (t, $J = 7.5$ Hz, 2H, CH_2), 3.08 (dd, $J = 15.0$ Hz, 6.6 Hz, 1H, CH_2), 3.37 (dd, $J = 15.0$ Hz, 4.8 Hz, 1H, CH_2), 3.61 (dt, $J = 13.5$ Hz, 7.5 Hz, 1H, CH_2), 3.82 (dt, $J = 13.5$ Hz, 7.5 Hz, 1H, CH_2), 4.04 (s, 5H, C_5H_5), 4.08 (dd, $J = 14.1$ Hz, 3.9 Hz, 1H, CH_2), 4.20–4.27 (m, 1H, CH), 4.28 (t,

J = 1.8 Hz, 2H, C_5H_4), 4.30 (dd, J = 14.1 Hz, 5.4 Hz, 1H, CH_2), 4.70 (t, J = 1.8 Hz, 2H, C_5H_4), 5.51 (d, J = 4.2 Hz, 1H, OH), 6.81 (s, 1H, 4-H), 7.15(d, J = 7.2 Hz, 1H, ArH), 7.19 (d, J = 8.1 Hz, 1H, ArH), 7.29 (t, J = 7.2 Hz, 1H, ArH), 7.38 (t, J = 7.5 Hz, 1H, ArH). HRMS calcd for $C_{25}H_{25}FFeN_3O_2$ $[M + H]^+$: 474.1280, found: 474.1246.

*6.4.9. Diethyl 1,1′-((2R,2′R)-(phenethylazanediyl)bis(2-hydroxypropane-3,1-diyl))bis(3-ferrocenyl-1H-pyrazole-5-carboxylate) [(R)-**3a**]*

Red oil. IR (KBr), ν/cm^{-1}: 3415 (O–H), 3088, 2939 (C–H), 1719 (C=O), 1457, 1258, 1085, 816, 764, 699, 486 (CpFeCp). ^{1}H NMR: δ 1.32 (t, J = 7.2 Hz, 6H, CH_3), 2.48–2.56 (m, 4H, CH_2), 2.58–2.71 (m, 4H, CH_2), 3.99–4.05 (m, 2H, CH), 4.01 (s, 10H, C_5H_5), 4.27 (t, J = 1.8 Hz, 4H, C_5H_4), 4.29 (q, J = 7.2 Hz, 4H, CH_2), 4.48–4.60 (m, 4H, CH_2), 4.74 (t, J = 1.8 Hz, 4H, C_5H_4), 4.81 (d, J = 4.8 Hz, 2H, OH), 6.97 (s, 2H, 4-H), 7.20 (m, 5H, ArH). HRMS calcd for $C_{46}H_{52}Fe_2N_5O_6$ $[M + H]^+$: 882.2616, found: 882.2600.

*6.4.10. (R)-ethyl 3-ferrocenyl-1-(2-hydroxy-3-(phenethylamino) propyl)-1H-pyrazole-5-carboxylate [(R)-**4a**]*

Red oil. IR (KBr), ν/cm^{-1}: 3420 (O–H), 3088, 2936, 2833 (C–H), 1719 (C=O), 1564 (C=N), 1457, 1384, 1260, 1085, 1006, 817, 699, 486 (CpFeCp). ^{1}H NMR: δ 1.33 (t, J = 7.2 Hz, 3H, CH_3), 2.65–2.72 (m, 2H, CH_2), 2.75–2.81 (m, 2H, CH_2), 2.86–2.94 (m, 2H, CH_2), 4.00–4.08 (m, 1H, CH), 4.04 (s, 5H, C_5H_5), 4.29 (t, J = 1.8 Hz, 2H, C_5H_4), 4.32 (q, J = 7.2 Hz, 2H, CH_2), 4.47 (dd, J = 13.5, 5.7 Hz, 1H, CH_2), 4.57 (dd, J = 13.5, 6.6 Hz, 1H, CH_2), 4.74 (t, J = 1.8 Hz, 2H, C_5H_4), 7.00 (s, 1H, 4-H), 7.17–7.31 (m, 5H, ArH). HRMS calcd for $C_{27}H_{32}FeN_3O_3$, $[M + H]^+$: 502.1793, found: 502.1786.

*6.4.11. (R)-7-hydroxy-5-(3-methoxyphenethyl)-2-phenyl-5,6,7,8-tetrahydropyrazolo[1,5-a][1,4]diazepin-4-one [(R)-**5**]*

White solid, yield 66%, mp 149–150 °C, $[\alpha]_D^{30}$ = −18.8 (c = 0.4, $CHCl_3$). IR (KBr), ν/cm^{-1}: 3422 (O–H), 2922 (C–H), 1665 (C=O), 1438, 1252, 1050, 772, 689. ^{1}H NMR: δ 2.90 (t, J = 7.5 Hz, 2H, CH_2), 3.08 (dd, J = 15.0 Hz, 6.9 Hz, 1H, CH_2), 3.41 (dd, J = 15.0 Hz, 5.1 Hz, 1H, CH_2), 3.59 (dt, J = 13.2 Hz, 7.5 Hz, 1H, CH_2), 3.75 (s, 3H, OCH_3), 3.87 (dt, J = 13.2 Hz, 7.5 Hz, 1H, CH_2), 4.16 (dd, J = 13.8 Hz, 3.0 Hz, 1H, CH_2), 4.20–4.29 (m, 1H, CH), 4.34 (dd, J = 13.8 Hz, 4.8 Hz, 1H, CH_2), 5.53 (d, J = 3.9 Hz, 1H, OH), 6.80 (d, J = 9.0 Hz, 1H, ArH), 6.86 (d, J = 6.9 Hz, 1H, ArH), 6.87 (s, 1H, 4-H), 7.17 (s, 1H, ArH), 7.23 (t, J = 7.8 Hz, 1H, ArH), 7.31 (t, J = 7.2 Hz, 1H, ArH), 7.41 (t, J = 7.5 Hz, 2H, ArH), 7.84 (d, J = 7.8 Hz, 2H, ArH). HRMS calcd for $C_{22}H_{24}N_3O_3$ $[M + H]^+$: 378.1818, found: 378.1806.

*6.4.12. (S)-7-hydroxy-5-(3-methoxyphenethyl)-2-phenyl-5,6,7,8-tetrahydropyrazolo[1,5-a][1,4]diazepin-4-one [(S)-**5**]*

White solid, yield 64%, mp 147–148 °C, $[\alpha]_D^{30}$ = +18.1 (c = 0.4, $CHCl_3$). IR (KBr), ν/cm^{-1}: 3422 (O–H), 2923 (C–H), 1665 (C=O), 1438, 1152, 1050, 772, 690. ^{1}H NMR: δ 2.90 (t, J = 7.5 Hz, 2H, CH_2), 3.08 (dd, J = 15.0 Hz, 7.2 Hz, 1H, CH_2), 3.41 (dd, J = 15.0 Hz, 5.1 Hz, 1H, CH_2), 3.59 (dt, J = 13.2 Hz, 7.5 Hz, 1H, CH_2), 3.75 (s, 3H, OCH_3), 3.87 (dt, J = 13.2 Hz, 7.5 Hz, 1H, CH_2), 4.16 (dd, J = 13.8 Hz, 3.3 Hz, 1H, CH_2), 4.20–4.29 (m, 1H, CH), 4.34 (dd, J = 13.8 Hz, 4.8 Hz, 1H, CH_2), 5.53 (d, J = 3.9 Hz, 1H, OH), 6.80 (d, J = 9.0 Hz, 1H, ArH), 6.86 (d, J = 7.2 Hz, 1H, ArH), 6.87 (s, 1H, 4-H), 7.17 (s, 1H, ArH), 7.23 (t, J = 7.8 Hz, 1H, ArH), 7.31 (t, J = 7.2 Hz, 1H, ArH), 7.41 (t, J = 7.5 Hz, 2H, ArH), 7.84 (d, J = 7.5 Hz, 2H, ArH). HRMS calcd for $C_{22}H_{24}N_3O_3$ $[M + H]^+$: 378.1818, found: 378.1807.

6.5. X-ray crystallography

Suitable single crystals of **2a** for X-ray structural analysis were obtained by slow evaporation of a solution of the solid in ethyl acetate at room temperature for 10 days. The crystals with approximate dimensions of 0.08 mm × 0.10 mm × 0.08 mm for **2a** were mounted on a Bruker Smart Apex II CCD equipped with a graphite monochromated MoKα radiation (λ = 0.71073 Å) by using φ and ω scan modes and the data were collected at 298(2) K. The structure of the crystal was solved by direct methods and refined by full-matrix least-squares techniques implemented in the SHELXTL-97 crystallographic software [65]. The non-hydrogen atoms were refined anisotropically. The hydrogen atoms bound to carbon were located by geometrical calculations, with their position and thermal parameters being fixed during the structure refinement. Molecular graphics were designed by using *XP* and *DIAMOND* 3.2.

6.6. Cell culture

A549, H322 and H1299 lung cancer cells were cultured in RPMI (Roswell Park Memorial Institute) 1640 medium at 37 °C with 5% CO_2, and 95% air, supplemented with 10% (v/v) bovine calf serum and 80 U/mL gentamicin. The cells were seeded onto 96-well plates or other appropriate dishes containing the medium at the cell density of 6250/cm^2.

6.7. Cell viability assay

Cells were seeded in 96-well plates. After 48 h, cells were treated with 0.1% DMSO (as control) or the compounds at indicated concentrations for specified time durations. The compounds were dissolved in DMSO as stock solution and applied to cells such that the final concentration of DMSO in the culture medium was below 0.1% (v/v). DMSO at a concentration of 0.1% (v/v) did not affect the viability of the cells. Cell viability was evaluated by sulforhodamine B (SRB) assay. Briefly, the medium was poured off and the cells were fixed by adding 100 μL of cold 10% trichloroacetic acid (TCA) and incubating for 1 h at 4 °C. The supernatant was discarded and then the plates were washed 5 times with deionized water. 50 μL of 0.4% (W/V) SRB solution in 1% acetic acid was added to each well and shaken for 5 min on a titer plate shaker. The plates were washed 5 times with 1% acetic acid and subsequently 100 μL of 10 mM unbuffered Tris base (pH 10.5) was added to dissolve the bound dye. After being mixed for 5 min on a microtiter plate shaker, optical densities were read at the wavelength of 510 nm using a SpectraMAX 190 microplate spectrophotometer (GMI Co., USA).

6.8. Hoechst 33258 staining to detect apoptosis

For A549, the living cells were stained with 10 μg/mL of Hoechst 33258 in the medium for 10 min at 37 °C. For H322 and H1299, cell fixation was done with 4% formaldehyde in phosphate buffered saline (PBS) for 10 min before staining with 2 μg/mL of Hoechst 33258 at 37 °C for 30 min. Subsequently, the cells were gently washed once with PBS, and were then observed under a fluorescence microscope (Nikon). The condensed DNA of apoptotic cells was identified by intense local staining in the nucleus, in contrast to diffused staining of DNA in normal cells. A minimum of 500 cells was counted, and each experiment was performed in triplicate.

6.9. Flow cytometry analysis of cell cycle distribution

Cells were harvested and then fixed with 70% ethanol, stained with 50 μg/mL propidium iodide (PI) containing 10 μg/mL RNase A at 4 °C for 1 h. The stained cells were analyzed using a FACS (Fluorescence Activated Cell Sorter) Calibur flow cytometer (BD Bioscience, USA). Cell cycle distribution was analyzed by ModiFit software (BD Bioscience, USA).

6.10. LDH assay

Lactate dehydrogenase (LDH) assay was performed on cells treated with 40 μM compounds, for 48 h using a LDH kit (Nanjing Jiancheng, China) according to the manufacturer's protocol. Light absorption was measured at 440 nm using a model Cintra 5 UV–vis spectrometer (GBC, Australia).

6.11. Statistical analysis

Data were presented as mean ± SD and analyzed by SPSS software. Pictures were processed with Photoshop software. Mean values were derived from at least three independent experiments. Differences at $p < 0.05$ were considered statistically significant.

Acknowledgments

This work was supported by National Natural Science Foundation of China (20972088 and 90813022) and The Independent Innovation Foundation of Shandong University (2009JC007).

Appendix A. Supplementary data

CCDC 885855 contain the supplementary crystallographic data for compound (*R*)-**2a**, these data can be obtained free of charge from The Cambridge Crystallographic Data Centre via http://www.ccdc.cam.ac.uk/conts/retrieving.html [or from the Cambridge Crystallographic Data Centre, 12 Union Road, Cambridge CB2 1EZ, UK; fax: +44(1223)336033; or e-mail: deposit@ccdc.cam.ac.uk].

References

[1] M. Bartucci, S. Svensson, P. Romania, R. Dattilo, M. Patrizii, M. Signore, S. Navarra, F. Lotti, M. Biffoni, E. Pilozzi, E. Duranti, S. Martinelli, C. Rinaldo, A. Zeuner, M. Maugeri-Saccà, A. Eramo, R.D. Maria, Therapeutic targeting of Chk1 in NSCLC stem cells during chemotherapy, Cell. Death Differ. 19 (2012) 768–778.
[2] L.G. Collins, C. Haines, R. Perkel, R.E. Enck, Lung cancer: diagnosis and management, Am. Fam. Physician 75 (2007) 56–63.
[3] G.M. Nitulescu, C. Draghici, A.V. Missir, Synthesis of new pyrazole derivatives and their anticancer evaluation, Eur. J. Med. Chem. 45 (2010) 4914–4919.
[4] S. Bondock, W. Fadaly, M.A. Metwally, Synthesis and antimicrobial activity of some new thiazole, thiophene and pyrazole derivatives containing benzothiazole moiety, Eur. J. Med. Chem. 45 (2010) 3692–3701.
[5] O. Rosati, M. Curini, M.C. Marcotullio, A. Macchiarulo, M. Perfumi, L. Mattioli, F. Rismondob, G. Cravotto, Synthesis, docking studies and anti-inflammatory activity of 4,5,6,7-tetrahydro-2*H*-indazole derivatives, Bioorg. Med. Chem. 15 (2007) 3463–3473.
[6] M.S. Christodoulou, S. Liekens, K.M. Kasiotis, S.A. Haroutounian, Novel pyrazole derivatives: synthesis and evaluation of anti-angiogenic activity, Bioorg. Med. Chem. 18 (2010) 4338–4350.
[7] D.M. Bailey, P.E. Hansen, A.G. Hlavac, E.R. Baizman, J. Pear, A.F. DeFelice, M.E. Feigensonf, 3,4-Diphenyl-1*H*-pyrazole-1-propanamine antidepressants, J. Med. Chem. 28 (1985) 256–260.
[8] B.P. Bandgar, S.S. Gawande, R.G. Bodade, N.M. Gawande, C.N. Khobragade, Synthesis and biological evaluation of a novel series of pyrazole chalcones as anti-inflammatory, antioxidant and antimicrobial agents, Bioorg. Med. Chem. 17 (2009) 8168–8173.
[9] S.R. Shih, T.Y. Chu, G.R. Reddy, S.N. Tseng, H.L. Chen, W.F. Tang, M.S. Wu, J.Y. Yeh, Y.S. Chao, J.T. Hsu, H.P. Hsieh, J.T. Horng, Pyrazole compound BPR1P0034 with potent and selective anti-influenza virus activity, J. Biomed. Sci. 17 (2010) 13.
[10] E. Strocchi, F. Fornari, M. Minguzzi, L. Gramantieri, M. Milazzo, V. Rebuttini, S. Breviglieri, C.M. Camaggi, E. Locatelli, L. Bolondi, M. Comes-Franchini, Design, synthesis and biological evaluation of pyrazole derivatives as potential multi-kinase inhibitors in hepatocellular carcinoma, Eur. J. Med. Chem. 48 (2012) 391–401.
[11] P. Puthiyapurayil, B. Poojary, C. Chikkanna, S.K. Buridipad, Design, synthesis and biological evaluation of a novel series of 1,3,4-oxadiazole bearing *N*-methyl-4-(trifluoromethyl)phenyl pyrazole moiety as cytotoxic agents, Eur. J. Med. Chem. 53 (2012) 203–210.
[12] I. Vujasinović, A. Paravić-Radičević, K. Mlinarić-Majerski, K. Brajša, B. Bertoša, Synthesis and biological validation of novel pyrazole derivatives with anticancer activity guided by 3D-QSAR analysis, Bioorg. Med. Chem. 20 (2012) 2101–2110.
[13] S. David, R.S. Perkins, F.R. Fronczek, S. Kasiri, S.S. Mandal, R.S. Srivastava, Synthesis, characterization, and anticancer activity of ruthenium-pyrazole complexes, J. Inorg. Biochem. 111 (2012) 33–39.
[14] S.L. Shen, J. Zhu, M. Li, B.X. Zhao, J.Y. Miao, Synthesis of ferrocenyl pyrazole-containing chiral aminoethanol derivatives and their inhibition against A549 and H322 lung cancer cells, Eur. J. Med. Chem. 54 (2012) 287–294.
[15] J. Quirante, D. Ruiz, A. Gonzalez, C. López, M. Cascante, R. Cortés, R. Messeguer, C. Calvis, L. Baldomà, A. Pascual, Y. Guérardel, B. Pradines, M. Font-Bardía, T. Calvet, C. Biot, Platinum(II) and palladium(II) complexes with (N, N′) and (C, N, N′)–ligands derived from pyrazole as anticancer and antimalarial agents: synthesis, characterization and in vitro activities, J. Inorg. Biochem. 105 (2011) 1720–1728.
[16] J.E. Westhead, H.D. Price, Quantitative assay of pyrazofurin, a new antiviral, antitumor antibiotic, Antimicrob. Agents Chemother. 5 (1) (1974) 90–91.
[17] O. Monasson, M. Ginisty, G. Bertho, C. Gravier-Pelletier, Y.L. Merrer, Efficient synthesis of polyfunctionalised enantiopure diazepanone scaffolds, Tetrahedron Lett. 48 (2007) 8149–8152.
[18] M. Igarashi, N. Nakagawa, N. Doi, S. Hattori, H. Naganawa, M. Hamada, Caprazamycin B, a novel anti-tuberculosis antibiotic, from *Streptomyces* sp. J. Antibiot. (Tokyo) 56 (2003) 580–583.
[19] M. Igarashi, Y. Takahashi, T. Shitara, H. Nakamura, H. Naganawa, T. Miyake, Y. Akamatsu, Caprazamycins, novel lipo-nucleoside antibiotics, from *Streptomyces* sp. J. Antibiot. (Tokyo) 58 (2005) 327–337.
[20] F. Sarabia, C. Vivar-García, C. García-Ruiz, L. Martín-Ortiz, A. Romero-Carrasco, Exploring the chemistry of epoxy amides for the synthesis of the 2″-epi-diazepanone core of liposidomycins and caprazamycins, J. Org. Chem. 77 (2012) 1328–1339.
[21] S. Hirano, S. Ichikawa, A. Matsuda, Structure–activity relationship of truncated analogs of caprazamycins as potential anti-tuberculosis agents, Bioorg. Med. Chem. 16 (2008) 5123–5133.
[22] B. Rosenberg, L. VanCamp, J.E. Trosko, V.H. Mansour, Platinum compounds: a new class of potent antitumour agents, Nature 222 (1969) 385–386.
[23] P.J. Dysona, G. Sava, Metal-based antitumour drugs in the post genomic era, Dalton Trans. 16 (2006) 1929–1933.
[24] G. Gasser, I. Ott, N. Metzler-Nolte, Organometallic anticancer compounds, J. Med. Chem. 54 (2011) 3–25.
[25] C. Wetzel, P.C. Kunz, M.U. Kassack, A. Hamacher, P. Böhler, W. Watjen, I. Ott, R. Rubbiani, B. Spingler, Gold(I) complexes of water-soluble diphos-type ligands: synthesis, anticancer activity, apoptosis and thioredoxin reductase inhibition, Dalton Trans. 40 (2011) 9212–9220.
[26] S.D. Köster, H. Alborzinia, S. Can, I. Kitanovic, S. Wölfl, R. Rubbiani, I. Ott, P. Riesterer, A. Prokop, K. Merza, N. Metzler-Nolte, A spontaneous gold(I)-azide alkyne cycloaddition reaction yields gold-peptide bioconjugates which overcome cisplatin resistance in a p53-mutant cancer cell line, Chem. Sci. 3 (2012) 2062–2072.
[27] Y. Geldmacher, K. Splith, I. Kitanovic, H. Alborzinia, S. Can, R. Rubbiani, M.A. Nazif, P. Wefelmeier, A. Prokop, I. Ott, S. Wölfl, I. Neundorf, W.S. Sheldrick, Cellular impact and selectivity of half-sandwich organo-rhodium(III) anticancer complexes and their organoiridium(III) and trichloridorhodium(III) counterparts, J. Biol. Inorg. Chem. 17 (2012) 631–646.
[28] F. Pelletier, V. Comte, A. Massard, M. Wenzel, S. Toulot, P. Richard, M. Picquet, P.L. Gendre, O. Zava, F. Edafe, A. Casini, P.J. Dyson, Development of bimetallic titanocene-ruthenium-arene complexes as anticancer agents: relationships between structural and biological properties, J. Med. Chem. 53 (2010) 6923–6933.
[29] M. Hanif, A.A. Nazarov, A. Legin, M. Groessl, V.B. Arion, M.A. Jakupec, Y.O. Tsybin, P.J. Dyson, B.K. Kepplera, C.G. Hartinger, Maleimide-functionalised organoruthenium anticancer agents and their binding to thiol-containing biomolecules, Chem. Commun. 48 (2012) 1475–1477.
[30] H. Amouri, J. Moussa, A.K. Renfrew, P.J. Dyson, M.N. Rager, L.-M. Chamoreau, Discovery, structure, and anticancer activity of an iridium complex of diselenobenzoquinone, Angew. Chem. Int. Ed. 49 (2010) 7530–7533.
[31] D. Pérez-Quintanilla, S. Gómez-Ruiz, Ž. Žižak, I. Sierra, S. Prashar, I. del Hierro, M. Fajardo, Z.D. Juranić, G.N. Kaluđerović, A new generation of anticancer drugs: mesoporous materials modified with titanocene complexes, Chem. Eur. J. 15 (2009) 5588–5597.
[32] A. Tzubery, E.Y. Tshuva, Cytotoxicity and hydrolysis of trans-Ti(IV) complexes of salen ligands: structure–activity relationship studies, Inorg. Chem. 51 (2012) 1796–1804.
[33] S.H. van Rijt, H. Kostrhunova, V. Brabec, P.J. Sadler, Functionalization of osmium arene anticancer complexes with (poly)arginine: effect on cellular uptake, internalization, and cytotoxicity, Bioconjug. Chem. 22 (2011) 218–226.
[34] Y.L.K. Tan, P. Pigeon, S. Top, E. Labbé, O. Buriez, E.A. Hillard, A. Vessières, C. Amatore, W.K. Leong, G. Jaouen, Ferrocenyl catechols: synthesis, oxidation chemistry and anti-proliferative effects on MDA-MB-231 breast cancer cells, Dalton Trans. 41 (2012) 7537–7549.
[35] J. Quirante, F. Dubar, A. González, C. Lopez, M. Cascante, R. Cortés, I. Forfar, B. Pradines, C. Biot, Ferrocene-indole hybrids for cancer and malaria therapy, J. Organomet. Chem. 696 (2011) 1011–1017.
[36] T.J. Kealy, P.L. Pauson, A new type of organo-iron compound, Nature 168 (1951) 1039–1040.
[37] D. Plazuk, S. Top, A. Vessières, M.-A. Plamont, M. Huché, J. Zakrzewski, A. Makal, K. Woźniak, G. Jaouen, Organometallic cyclic polyphenols derived from 1,2-(α-keto tri or tetra methylene) ferrocene show strong

antiproliferative activity on hormone-independent breast cancer cells, Dalton Trans. 39 (2010) 7444–7450.
[38] D. Dive, C. Biot, Ferrocene conjugates of chloroquine and other antimalarials: the development of ferroquine, a new antimalarial, ChemMedChem 3 (2008) 383–391.
[39] A. Mahajan, L. Kremer, S. Louw, Y. Guéradel, K. Chibale, C. Biot, Synthesis and in vitro antitubercular activity of ferrocene-based hydrazones, Bioorg. Med. Chem. Lett. 21 (2011) 2866–2868.
[40] R.D. Miao, J. Wei, M.H. Lv, Y. Cai, Y.P. Du, X.P. Hui, Q. Wang, Conjugation of substituted ferrocenyl to thiadiazine as apoptosis-inducing agents targeting the Bax/Bcl-2 pathway, Eur. J. Med. Chem. 46 (2011) 5000–5009.
[41] A.C. de Oliveira, E.A. Hillard, P. Pigeon, D.D. Rocha, F.A. Rodrigues, R.C. Montenegro, L.V. Costa-Lotufo, M.O. Goulart, G. Jaouen, Biological evaluation of twenty-eight ferrocenyl tetrasubstituted olefins: cancer cell growth inhibition, ROS production and hemolytic activity, Eur. J. Med. Chem. 46 (2011) 3778–3787.
[42] P.Z. Li, Z.Q. Liu, Ferrocenyl-substituted curcumin: can it influence antioxidant ability to protect DNA? Eur. J. Med. Chem. 46 (2011) 1821–1826.
[43] G.M. Maguene, J. Jakhlal, M. Ladyman, A. Vallin, D.A. Ralambomanana, T. Bousquet, J. Maugein, J. Lebibi, L. Pélinski, Synthesis and antimycobacterial activity of a series of ferrocenyl derivatives, Eur. J. Med. Chem. 46 (2011) 31–38.
[44] F. Wei, B.X. Zhao, B. Huang, L. Zhang, C.H. Sun, W.L. Dong, D.S. Shinc, J.Y. Miao, Design, synthesis, and preliminary biological evaluation of novel ethyl 1-(2′-hydroxy-3′-aroxypropyl)-3-aryl-1*H*-pyrazole-5-carboxylate, Bioorg. Med. Chem. Lett. 16 (2006) 6342–6347.
[45] Y. Xia, Z.W. Dong, B.X. Zhao, X. Ge, N. Meng, D.S. Shin, J.Y. Miao, Synthesis and structure–activity relationships of novel 1-arylmethyl-3-aryl-1*H*-pyrazole-5-carbohydrazide derivatives as potential agents against A549 lung cancer cells, Bioorg. Med. Chem. 15 (2007) 6893–6899.
[46] Y.S. Xie, X.H. Pan, B.X. Zhao, J.T. Liu, D.S. Shin, J.H. Zhang, L.W. Zheng, J. Zhao, J.Y. Miao, Synthesis, structure characterization and preliminary biological evaluation of novel 5-alkyl-2-ferrocenyl-6,7-dihydropyrazolo[1,5-a]pyrazin-4(5*H*)-one derivatives, J. Organomet. Chem. 693 (2008) 1367–1374.
[47] X.H. Pan, X. Liu, B.X. Zhao, Y.S. Xie, D.S. Shin, S.L. Zhang, J. Zhao, J.Y. Miao, 5-Alkyl-2-ferrocenyl-6,7-dihydropyrazolo[1,5-a]pyrazin-4(5*H*)-one derivatives inhibit growth of lung cancer A549 cell by inducing apoptosis, Bioorg. Med. Chem. 16 (2008) 9093–9100.
[48] C.D. Fan, B.X. Zhao, F. Wei, G.H. Zhang, W.L. Dong, J.Y. Miao, Synthesis and discovery of autophagy inducers for A549 and H460 lung cancer cells, novel 1-(2′-hydroxy-3′-aroxypropyl)-3-aryl-1*H*-pyrazole-5-carbohydrazide derivatives, Bioorg. Med. Chem. Lett. 18 (2008) 3860–3864.
[49] B.X. Zhao, L. Zhang, X.S. Zhu, M.S. Wan, J. Zhao, Y. Zhang, S.L. Zhang, J.Y. Miao, Synthesis and discovery of a novel pyrazole derivative as an inhibitor of apoptosis through modulating integrin β4, ROS, and p53 levels in vascular endothelial cells, Bioorg. Med. Chem. 16 (2008) 5171–5180.
[50] J.H. Zhang, C.D. Fan, B.X. Zhao, D.S. Shin, W.L. Dong, Y.S. Xie, J.Y. Miao, Synthesis and preliminary biological evaluation of novel pyrazolo[1,5-a] pyrazin-4(5*H*)-one derivatives as potential agents against A549 lung cancer cells, Bioorg. Med. Chem. 16 (2008) 10165–10171.
[51] Y. Xia, C.D. Fan, B.X. Zhao, J. Zhao, D.S. Shin, J.Y. Miao, Synthesis and structure–activity relationships of novel 1-arylmethyl-3-aryl-1*H*-pyrazole-5-carbohydrazide hydrazone derivatives as potential agents against A549 lung cancer cells, Eur. J. Med. Chem. 43 (2008) 2347–2353.
[52] L.W. Zheng, L.L. Wu, B.X. Zhao, W.L. Dong, J.Y. Miao, Synthesis of novel substituted pyrazole-5-carbohydrazide hydrazone derivatives and discovery of a potent apoptosis inducer in A549 lung cancer cells, Bioorg. Med. Chem. 17 (2009) 1957–1962.
[53] S. Lian, H. Su, B.X. Zhao, W.Y. Liu, L.W. Zheng, J.Y. Miao, Synthesis and discovery of pyrazole-5-carbohydrazide *N*-glycosides as inducer of autophagy in A549 lung cancer cells, Bioorg. Med. Chem. 17 (2009) 7085–7092.
[54] X.L. Ding, H.Y. Zhang, L. Qi, B.X. Zhao, S. Lian, H.S. Lv, J.Y. Miao, Synthesis of novel pyrazole carboxamide derivatives and discovery of modulators for apoptosis or autophagy in A549 lung cancer cells, Bioorg. Med. Chem. Lett. 19 (2009) 5325–5328.
[55] L.W. Zheng, J.H. Shao, B.X. Zhao, J.Y. Miao, Synthesis of novel pyrazolo[1,5-a]pyrazin-4(5*H*)-one derivatives and their inhibition against growth of A549 and H322 lung cancer cells, Bioorg. Med. Chem. Lett. 21 (2011) 3909–3913.
[56] L.W. Zheng, J. Zhu, B.X. Zhao, Y.H. Huang, J. Ding, J.Y. Miao, Synthesis, crystal structure and biological evaluation of novel 2-(5-(hydroxymethyl)-3-phenyl-1*H*-pyrazol-1-yl)-1-phenylethanol derivatives, Eur. J. Med. Chem. 45 (2010) 5792–5799.
[57] H.S. Lv, X.Q. Kong, Q.Q. Ming, X. Jin, J.Y. Miao, B.X. Zhao, Synthesis of 5-benzyl-2-phenylpyrazolo[1,5-a]pyrazin-4,6(5*H*,7*H*)-dione derivatives and discovery of an apoptosis inducer for H322 lung cancer cells, Bioorg. Med. Chem. Lett. 22 (2012) 844–849.
[58] Y.S. Xie, H.L. Zhao, H. Su, B.X. Zhao, J.T. Liu, J.K. Li, H.S. Lv, B.S. Wang, D.S. Shin, J.Y. Miao, Synthesis, single-crystal characterization and preliminary biological evaluation of novel ferrocenyl pyrazolo[1,5-a]pyrazin-4(5*H*)-one derivatives, Eur. J. Med. Chem. 45 (2010) 210–218.
[59] P. Seiler, J.D. Dunitz, The structure of triclinic ferrocene at 101, 123 and 148 K, Acta Crystallogr. B 35 (1979) 2020–2032.
[60] G. Tabbì, C. Cassino, G. Cavigiolio, D. Colangelo, A. Ghiglia, I. Viano, D. Osella, Water stability and cytotoxic activity relationship of a series of ferrocenium derivatives. ESR insights on the radical production during the degradation process, J. Med. Chem. 45 (2002) 5786–5796.
[61] A. Vessières, S. Top, W. Beck, E. Hillard, G. Jaouen, Metal complex SERMs (selective oestrogen receptor modulators). The influence of different metal units on breast cancer cell antiproliferative effects, Dalton Trans. 4 (2006) 529–541.
[62] I. Damljanović, M. Čolović, M. Vukićević, D. Manojlović, N. Radulović, K. Wurst, G. Laus, Z. Ratković, M. Joksović, R.D. Vukićević, Synthesis, spectral characterization and electrochemical properties of 1*H*-3-(*o*-, *m*- and *p*-ferrocenylphenyl)-1-phenylpyrazole-4-carboxaldehydes, J. Organomet. Chem. 694 (2009) 1575–1580.
[63] J. Skiba, A. Rajnisz, K.N. de Oliveira, I. Ott, J. Solecka, K. Kowalski, Ferrocenyl bioconjugates of ampicillin and 6-aminopenicillinic acid-synthesis, electrochemistry and biological activity, Eur. J. Med. Chem. 57 (2012) 234–239.
[64] Z.A. Stewart, M.D. Westfall, J.A. Pietenpol, Cell-cycle dysregulation and anticancer therapy, Trends Pharmacol. Sci. 24 (2003) 139–145.
[65] G.M. Sheldrick, A short history of SHELX, Acta. Crystallogr. A. Found. Crystallogr. 64 (2008) 112–122.